



1 **Brief Communication**

2 **Co-seismic displacement on October 26 and 30, 2016 (M_w 5.9 and 6.5) -**
3 **earthquakes in central Italy from the analysis of discrete GNSS network**

4
5 De Guidi Giorgio¹, Vecchio Alessia¹, Brighenti Fabio¹, Caputo Riccardo^{2,3}, Carnemolla Francesco¹, Di
6 Pietro Adriano¹, Lupo Marco¹, Maggini Massimiliano², Marchese Salvatore¹, Messina Danilo¹, Monaco
7 Carmelo¹, Naso Salvatore¹
8

9 ¹) Department of Biological Geological and Environmental Sciences, University of Catania, Italy

10 ²) Department of Physics and Earth Sciences, University of Ferrara, Italy

11 ³) Research and Teaching Center for Earthquake Geology, Tyrnavos, Greece

12 *Corresponding author:* G. De Guidi (deguidi@unict.it)

13

14

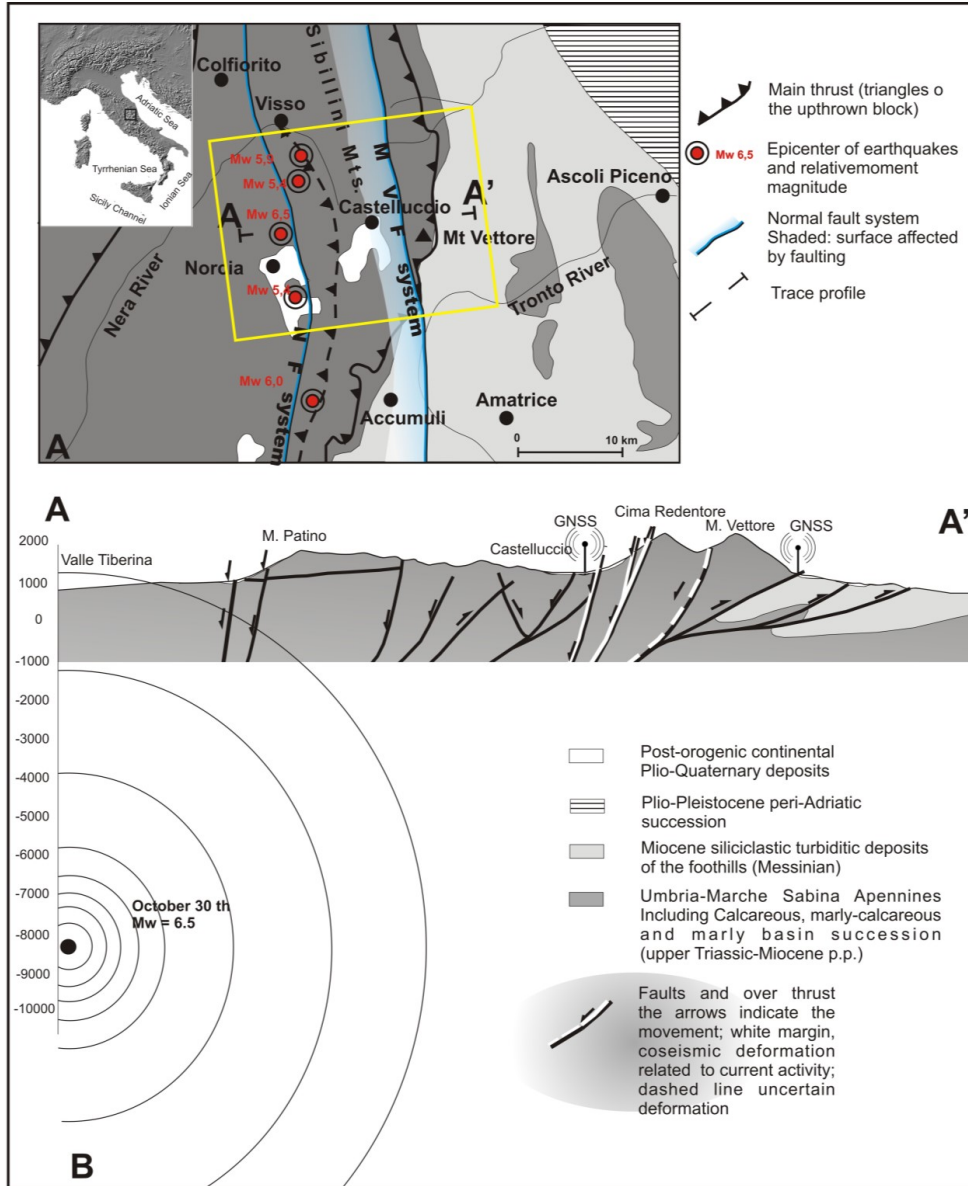
15 **1 - Abstract**

16 On October 26th 2016, immediately north of the epicentral area affected by the M_w 6.0, August 24th
17 earthquake, a strong earthquake ($M_w = 5.9$), with a focal mechanism showing *W*-dipping normal faulting,
18 occurred at the boundary between Marche and Umbria regions (central Apennines, Italy). Four days later
19 (on October 30th), the main-shock ($M_w = 6.5$) of the whole seismic sequence occurred in the same area. The
20 central Apennines are characterized by northeast-verging thrust-propagation folds, involving Mesozoic-
21 Tertiary sedimentary successions. During the 2016 sequence, coseismic deformation has been recorded at
22 the rear of the Sibillini Thrust which separates the main mountain chain from the Marche-Abruzzi foothills
23 (Fig. 1). This contractional structure has been partly dissected and/or inverted by NNW-SSE trending
24 Quaternary normal and oblique-slip faults. The major event (October 30) induced extensive geological
25 effects at the surface and structural damages in the broader epicentral area up to a distance of 30 km.
26 According to the report of the Istituto Nazionale di Geofisica e Vulcanologia (SUMMARY REPORT ON THE 30
27 OCTOBER, 2016 EARTHQUAKE IN CENTRAL ITALY M_w 6.5, Gruppo di Lavoro INGV sul Terremoto in centro
28 Italia 10 November 2016), the hypocenter of major event was located at 42.8322°N, 13.1107°E at a depth
29 of 9.2 km (Figs. 1 and 2). Following the August seismic events, we installed five new geodetic points located
30 on both sides of the principal fracture zone and carried out two campaigns of GNSS measurements, the first
31 one at the end of September (30-09/02-10, 2016), the second one early November (11/13-11, 2016) that
32 covered the period of the October events.

33 In this brief communication, we provide the results of our geodetic campaigns that registered the co-
34 seismic displacement occurred in the period between doy (day of year) 2016/274 and doy 2016/318,
35 therefore documenting the two latter major shocks. We also compare our results with the available surface
36 deformation field of the broader area obtained on the basis of the DInSAR technique and particularly the
37 elaboration realized by CNR-IREA of Sentinel-1 radar imaging of Copernicus European Program of 26/10 -
38 1/11 (http://www.irea.cnr.it/index.php?option=com_k2&view=item&id=761:nuovi-risultati-sul-terremoto-del-30-ottobre-2016-ottenuti-dai-radar-dei-satelliti-sentinel-1). The comparison shows an overall good fit.
39 It's worth to note that these earthquakes occurred in a sector of the Central Apennines characterized by
40 high geodetic strain-rates (e.g., D'Agostino 2014), where several continuous GNSS stations are operating.
41
42



43



44
 45
 46
 47
 48
 49

Fig. 1 A) Simplified seismotectonic map of central Apennines; B) east-west geological profile; for the trace see the A map. The main geostructural features are reported (Pierantoni et al., 2013, modified)

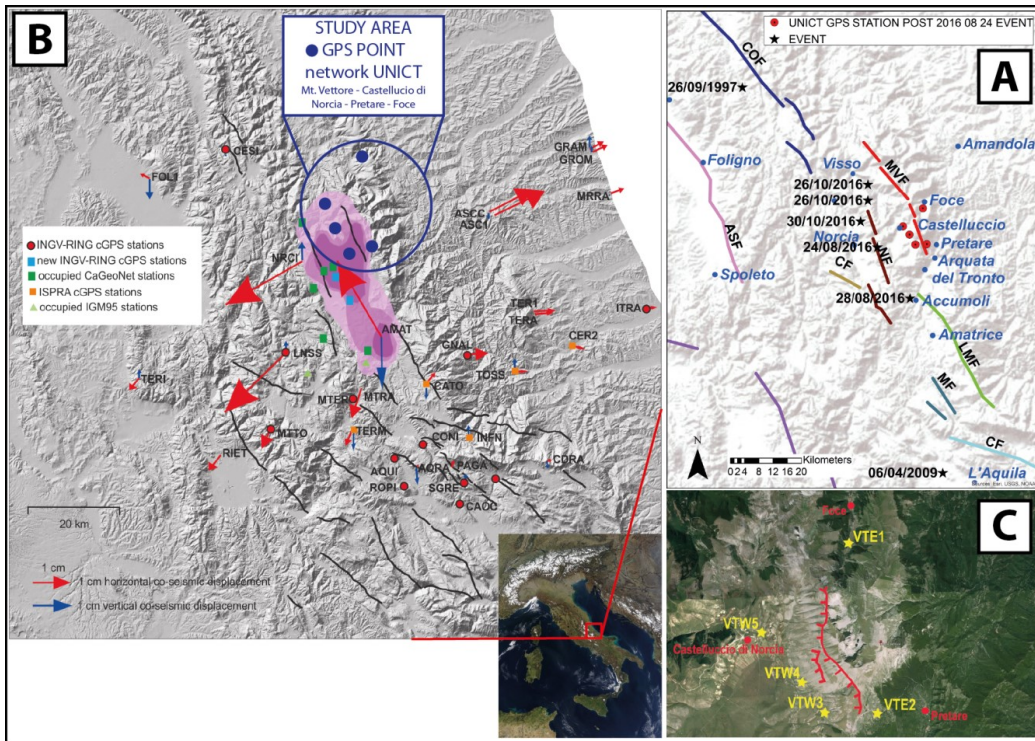
Active faults

50
 51
 52
 53

According to many authors in the area affected by the recent earthquakes, the main thrust-related anticlines and associated reverse faults characterizing have been dissected and/or inverted by NNW-SSE trending Quaternary normal and oblique-slip faults (Figs. 1 and 2), in particular by the Norcia Fault system (NF) (Calamita and Pizzi, 1992; Calamita et al., 1982; 1995; 1999; 2000; Blumetti et al., 1990; Blumetti,



54 1995; Brozzetti and Lavecchia, 1994; Cello et al., 1998; Galadini and Galli, 2000; Pizzi and Scisciani, 2000;
 55 Pizzi et al., 2002; Galadini, 2006; Gori et al., 2007) and by the Mt. Vettore Fault system (MVF) (Calamita and
 56 Pizzi, 1991; Coltorti and Farabollini, 1995; Cello et al., 1997; Pizzi et al., 2002; Galadini and Galli, 2003; Pizzi
 57 and Galadini, 2009) (Figs. 1 and 2). Conversely, Pierantoni et al. (2013) suggest that the major Mt. Sibillini
 58 Thrust has not yet been dissected by Quaternary normal faulting though some fresh morphological scarps
 59 with free faces in the carbonate bedrock and/or affecting recent slope deposits have been observed and
 60 attributed to the local seismic activity.
 61



62
 63
 64 *Fig. 2 – A) Digital Elevation Model with shaded relief of central Apennines showing the active fault system. ASF: Assisi*
 65 *Fault; COF: Colfiorito Fault; CF: Cascia Fault; MVF: Mt. Vettore Fault; NF: Norcia Fault; LMF: Laga Mts. Fault; MF: faults*
 66 *of the Montereale basin and mains events since 1997. B) The figure shows the horizontal (red arrows) and vertical*
 67 *(blue arrows) consensus co-seismic displacements (with 68% confidence errors), together with the August 24th, Mw 6,0*
 68 *mainshock (yellow star) and aftershocks (colored as a function of depth) from <http://iside.rm.ingv.it>; and the position*
 69 *of UNICT_NET GPS C). Red coloured segments represent the October 30th, coseismic deformation.*

70
 71 After the August 24th, 2016 mainshock, field observations (EMERGEO W.G., 2016) showed that only the
 72 southern segment of the Monte Vettore Fault system was reactivated in the northern sector of the
 73 epicentral area (Fig. 2C). So, a continuous alignment of newly formed coseismic ruptures was mapped for
 74 more than 5.2 km; conversely, in the southern sector, only few sparse observations of discontinuous
 75 (maximum 300 m-long) unclear ground ruptures with small displacements have been observed (EMERGEO
 76 W.G., 2016).
 77 After the second mainshock (October 30), brittle deformation reached the surface producing evident
 78 ground ruptures along the Mt. Vettore – Mt. Bove Fault systems. A continuous rupture was mapped for a



79 minimum length of 15 km between the Castelluccio di Norcia and Ussita (EMERGEO W.G., 2016) (Fig. 2).
80 The coseismic rupture occurred along distinct fault splays of the fracture system. For example, along the
81 western slope of Mt. Vettore three main west dipping branches were activated together with two
82 antithetic structures (Figs. 1 and 2). The vertical offset reaches 2 m along the main west dipping fault splay,
83 where the slickensides show a prevalent vertical component of motion. Vertical displacements of few
84 centimetres were also recorded along the antithetic tectonic structure bordering to the west the
85 Castelluccio plain, about 6-7 km far from the main ground rupture (Fig. 2).

86
87

88 **Implementation and Analysis of UNICT discrete GPS stations**

89

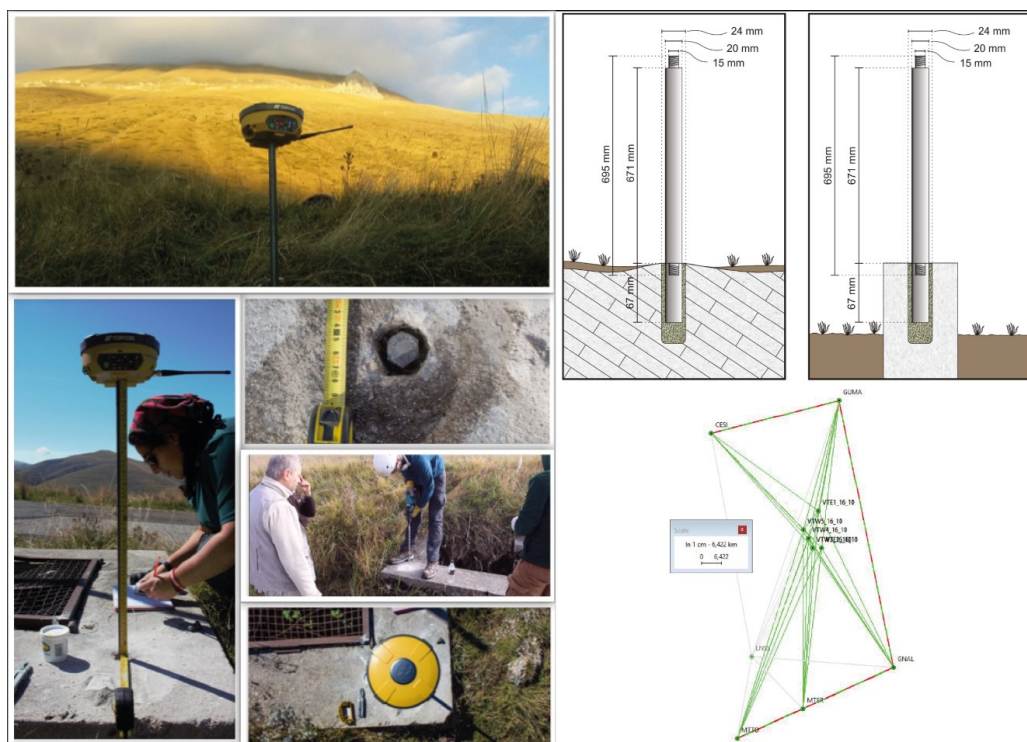
90 Following the August, 24th, M_w 6.0 earthquake, the GEOmatic Working Group of the Catania University
91 (UNICT) in collaboration with the SpinOff EcoStat s.r.l. and researches of the Ferrara University, started a
92 detailed monitoring of ground deformation in the epicentral area using the Global Navigation Satellite
93 System (GNSS) technique. For this aim, five GNSS stations have been installed on benchmarks built by the
94 working group and here referred to as UNICT_NET network (Fig. 3). These new stations have been realized
95 taking into account the following criteria:

- 96 I. the distribution of the existing permanent and discrete measurement benchmarks belonging to
97 different networks that were active before the event of 24 August (IGM; RING; CAGEONET; DPC;
98 ISPRA) (Fig. 2B).
- 99 II. the seismotectonic setting of the area in relation to the macroseismic data and to the reactivated
100 structures (Figs. 1 and 2);
- 101 III. surface and deep geometry of the major faults related to tectonic setting (Fig. 1B).
- 102 IV. the non-occurrence of possible instabilities in both static and dynamic conditions in sites where the
103 new benchmarks are built.

104

105 Based on the above criteria, the working group installed the benchmarks at the bottom of both western
106 and eastern slopes of Mt. Vettore, within an area about 8 km-long and 5 km-wide in the N-S and E-W
107 directions, respectively. The distribution of the benchmarks was planned for depicting the principal
108 deformation zone developed as a consequence of the August 24th, event (Fig 2 and 3) and particularly with
109 points:

- 110 I. much closer to the epicentral area than the already existing ones belonging to other networks
111 (Fig. 2B);
- 112 II. characterized by equivalent distances from the reactivated Mt. Vettore Fault segments (Fig. 2);
- 113 III. within a distance of 30 km from the closest permanent network points that have been not affected
114 by deformation, therefore allowing a rigorous elaboration during the post processing phases (Fig.
115 3).



116

117 *Fig. 3 Synoptic picture showing installation, measurement and processing phases of the UNICT_NET.*

118

119 The realization of GPS monument on the UNICT benchmarks consists of the following steps:

120

- I. selection of a suitable point, corresponding to a massive rocky outcrop or a man-made monument with foundation; these sites must be also free of structures or other natural elements in the surroundings that may constitute a perturbation during recording;
- 121
- 122
- 123 II. testing of GPS signal reception by short-term exams, and control of parameters set by the quality check carried out by software TEQC (<http://www.unavco.org/software/data-processing/teqc/teqc.html>);
- 124
- 125
- 126 III. implementation of the hole for housing the bushing and check of its verticality; the hole has a diameter of 35 mm and a depth of 100 mm, it is realized through small-sized battery-powered equipment (Makita DHR243 hammer drill) (Fig. 3);
- 127
- 128
- 129 IV. fixing and anchoring of the knurled steel bushing (length 67 mm and diameter 20 mm), with bi-component resins or quick-setting cements (Fig. 3);
- 130
- 131 V. following the cementation to the artefact or to rocky outcrop, a male-male threaded bar can be screwed in until end of stroke; the height could be variable and this fact will be considered in the data processing. We have used a threaded bar 670 mm-high. (Fig. 3).
- 132
- 133

134

The GPS monument is thus completed with a GNSS receiver TOPCON, mounting a HiPer V antenna, characterized by 226 channels and position accuracy with band L1+L2 in Static mode of 3 mm + 0,1 ppm (horizontal) and 3,5 mm + 0,4 ppm (vertical). All registrations last six hours in static mode.

135

136

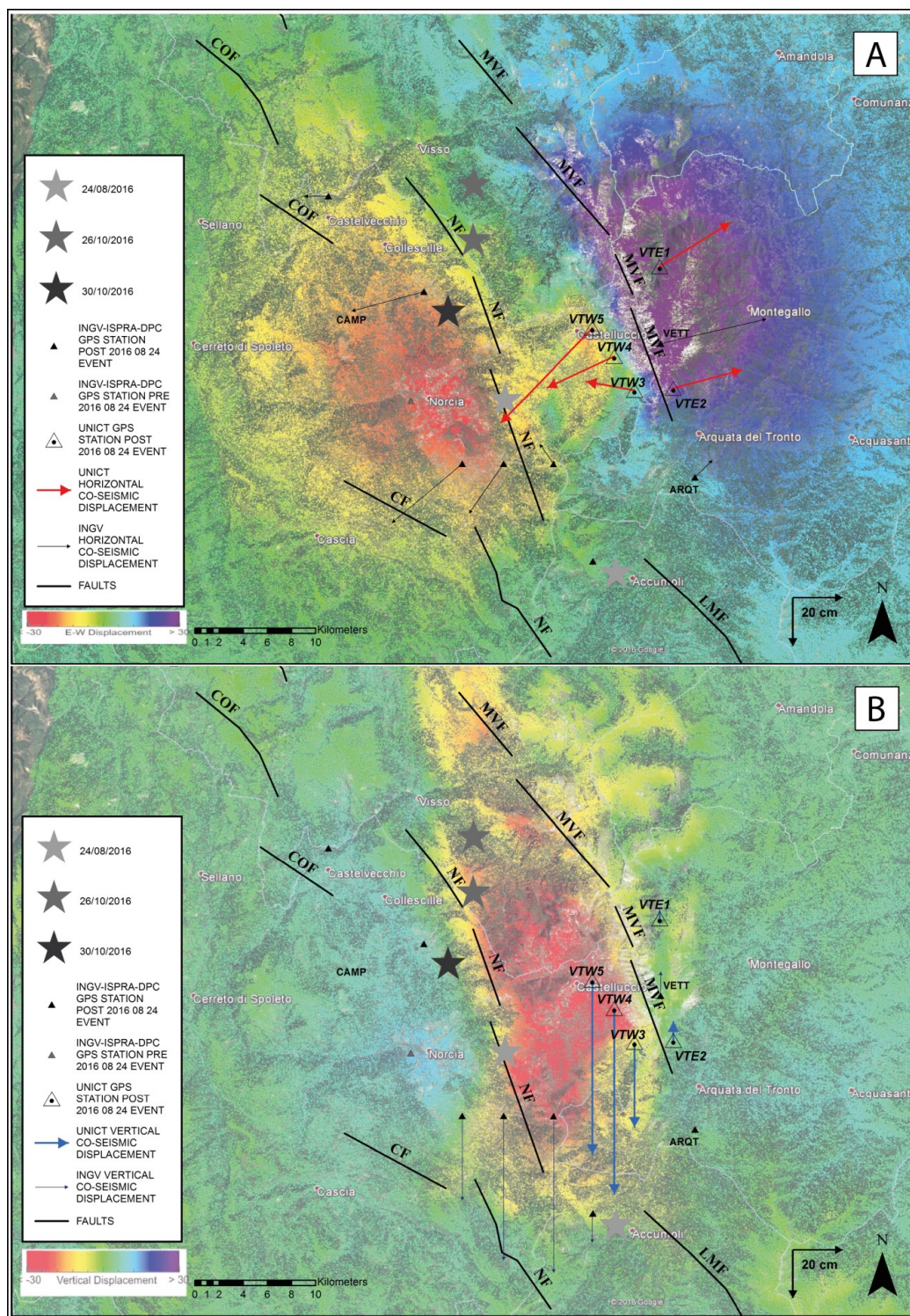


137 Following the August 24th, event, at the end of September 2016 the working group have started the first
138 survey campaign with the installation of five UNICT benchmarks: two stations have been located east of the
139 Mt. Vettore fault (VTE1,VTE2), the other three (VTW3,VTW4, VTW5) west of the fault (Figs. 3 and 4). During
140 November 2016 (*i.e.* after the October 30th event), a second field campaign was carried out following the
141 same procedure and using the same instrumentation. The second set of measurements allowed to record
142 the co-seismic displacement caused by both the M_w 5.9 and M_w 6.5 events of October 26th and 30th,
143 respectively.

144 The data from survey-mode GNSS stations have been downloaded and processed using TOPCON Magnet
145 analysis software evaluating co-seismic solution.

146 For the analyses we referred to the measurement of a stable reference frame of five GNSS stations
147 belonging to the RING (Rete Integrata Nazionale GPS) network, with a maximum baseline length of 30 km
148 using stations CESI, GNAL, GUMA, MTER and MTTO (Figs. 3 and 4). Data processing has been carried out
149 with adjustment by Least Squares and a TAU Criterion.

150





152 Fig. 4 The two color-coded maps show the E-W (a) and VERTICAL (b) displacement distribution obtained by the DInSAR
 153 technique (http://www.irea.cnr.it/index.php?option=com_k2&view=item&id=761:nuovi-risultati-sul-terremoto-del-30-ottobre-2016-ottenuti-dai-radar-dei-satelliti-sentinel-1), while the red and blu arrows represent the consensus pre-, co-
 154 , and post-seismic displacements (with 95% confidence errors) on the basis of the GNSS UNICT network. Epicenters of
 155 the October, 26th and 30th M_w 5.9 - 6.5 and of the August, 24th, M_w 6 events are also shown (<http://ring.gm.ingv.it>) as
 156 well as the position and relative measured vector of the CaGeoNet stations (Anzidei et al. 2008; Galvani et al., 2012),
 157 the IGM95 benchmarks (<http://www.igmi.org/geodetica/>) re-occupied by ISPRA (www.isprambiente.gov.it) after the
 158 mainshock and the continuous GPS stations managed by ISPRA and the Civil Protection Department (DPC).
 159
 160

SITE ID	MARKER NUMBER	lon °E	lat °N	Hei (m)	Ground Distance (m)	Delta Ell. (m)	Network
VTE1	FOCE_SENTIERO	13° 15' 58,16654"	42° 51' 55,80640"	1091,690	0,344	0,034	UNICT
VTE2	PRETARE	13° 16' 33,92314"	42° 47' 55,33158"	1049,532	0,294	0,077	UNICT
VTW3	QUARTUCCIOLO	13° 14' 47,12569"	42° 47' 55,33427"	1475,886	0,203	-0,352	UNICT
VTW4	COLLE CURINA	13° 13' 55,72696"	42° 48' 58,38892"	1371,543	0,308	-0,771	UNICT
VTW5	CASTELLUCCIO_VALLE	13° 12' 56,91921"	42° 49' 53,65362"	1375,999	0,547	-0,722	UNICT

161
 162 Tab 1 - Co-seismic displacements (in m) estimated for the GNSS stations of the UNICT network on both sides of the
 163 principal deformation zone of the Monte Vettore Fault characterized by a mean distance lower than 4 km from the
 164 PDZ). The table can be download as ASCII file on the INGVING web page (<http://ring.gm.ingv.it>). The first column indicates the GNSS station name ; lon: longitude (°E), lat: latitude (°N), Hei: station height (in meters). Ground distance and vertical co-seismic displacements and corresponding
 165 uncertainties, in m. The last column indicates the GNSS/GPS network.
 166
 167
 168

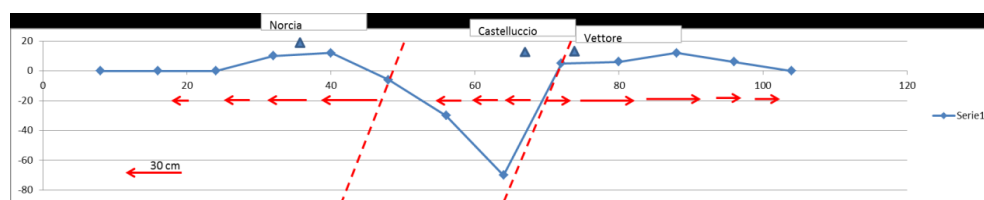
169 Concluding remarks

170 Based on the GNSS technique, a detailed monitoring of the ground deformation occurred in the
 171 surroundings of the Mt. Vettore Fault segment, partially reactivated by the August 24th (M_w 6.0), has been
 172 carried out. This foresight action allowed us to record the second (strongest) event (M_w 6.5) of October
 173 30th, 2016. On the basis of the laws and models on stress-triggering theory (Stein et al., 1999; Steacy et al.,
 174 2005), we have identified the specific fault zone most vulnerable to future seismic events just north of the
 175 fault segment reactivated on 24th August (Figs. 2B and 4). Consequently in order to measure the post
 176 seismic deformation and to record a potential migration of the coseismic process, we have placed the GNSS
 177 benchmarks, both east and west of the northern-central segment of the Mt. Vettore Fault system, close to
 178 other benchmarks located before the second seismic event by other research groups (IGM; RING;
 179 CAGEONET; DPC; ISPRA). The measured deformation (with 95% confidence errors) is characterised by
 180 horizontal and vertical movement. From north to south, the east benchmarks indicated 344 mm eastward
 181 horizontal displacement and 34 mm upward (VTE1), 294 mm eastward horizontal displacement and 77 mm
 182 upward component of motion (VTE2); on the contrary, all the three western benchmarks have recorded
 183 westward horizontal displacement and downthrown component of motion: 547 mm and -722 mm (VTW5);
 184 308 mm and -771 mm (VTW4); 203 mm and -352 mm (VTW3). So, the maximum horizontal displacement
 185 was 891 mm in correspondence of the northern sector of the Mt. Vettore fault segment, while the
 186 maximum vertical displacement was 848 mm.

187 In conclusion, the comparison between our results and the displacement distribution obtained with DInSAR
 188 techniques, and other GNSS stations, active before the second seismic event (Fig. 4), indicate the
 189 consistency of the data.



190 Moreover, the semi-quantitative analysis along the west-east deformation transect (Fig. 5), indicate an
191 anomalous variation of both horizontal and vertical deformation, suggesting a possible “seismic efficiency”
192 of the Norcia fault system, located to the west of the Mt. Vettore fault system. We have placed new
193 benchmarks in strategic positions for monitoring pre, inter and post-seismic deformation.
194



195
196
197
198
199
200
201
202
203 *Fig. 5 Semi-quantitative comparison between west-east deformation transects obtained by DInSAR techniques and our*
204 *GNSS measurements (see fig 4)*

205
206 **Acknowledgments** This paper was carried out with the financial support of the University of Catania (FIR
207 2014 Project Code 2C7D79, Scientific Supervisor: G. De Guidi) and University Spin Off of Catania EcoStat
208 s.r.l.

209 References

- 210
211
212 Anzidei, M., P. Baldi, and E. Serpelloni, 2008. The coseismic ground deformations of the 1997 Umbria-
213 Marche earthquakes: A lesson for the development of new GPS networks, *Ann. Geophys.*, 51(2–3), 27–43.
214
215 Blumetti A.M., 1995. Neotectonic investigations and evidence of paleoseismicity in the epicentral area of
216 the January-February 1703, Central Italy, earthquakes. In: Serva, L. & Slemmons, D. B., (eds.): *Perspectives*
217 *in paleoseismology*. Association of Engineering Geologists, spec. publ. 6, 83-100.
218
219 Blumetti A.M., Dramis F., Gentili B., Pambianchi G., 1990. La struttura di M. Alvagnano-Castel Santa Maria
220 nell’area nursina: aspetti geomorfologici e sismicità storica. *Rend. Soc. Geol. It.*, 13, 71-76.
221
222 Brozzetti F., Lavecchia G., 1994. Seismicity and related extensional stress field; the case of the Norcia
223 seismic zone (central Italy). *Annales Tectonicae* 8, 36–57
224
225 Calamita F., Pizzi A., 1992. Tettonica quaternaria nella dorsale appenninica umbro-marchigiana e bacini
226 intrappenninici associati. *Studi Geologici Camerti*, spec. vol. 1992/1, 17-25.
227
228 Calamita F., Coltorti M., Deiana G., Dramis F., Pambianchi G., 1982. Neotectonic evolution and
229 geomorphology of the Cascia and Norcia depression (Umbria-Marche Apennine). *Geografia Fisica e*
230 *Dinamica Quaternaria*, 5, 263-276.
231
232 Calamita F., Pizzi A., Romano A., Roscioni M., Scisciani V., Vecchioni G., 1995. La tettonica quaternaria nella
233 dorsale appenninica umbro-marchigiana: una deformazione progressiva non coassiale. *Studi Geol. Camerti*,
234 vol. spec.1995/1, 203-223.
235



- 236 Calamita F., Coltorti M., Pieruccini P., Pizzi A., 1999. Evoluzione strutturale e morfogenesi plio-quadernaria
237 dell'appennino umbro-marchigiano tra il preappennino umbro e la costa adriatica. *Bollettino della Società*
238 *Geologica Italiana*, 118, 125-139.
- 239
- 240 Calamita F., Coltorti M., Piccinini D., Pierantoni P.P., Pizzi A., Ripepe M., Scisciani V., Turco E., 2000.
241 Quaternary faults and seismicity in the Umbro-Marchean Apennines (central Italy). *Journal of Geodynamics*
242 29, 245–264.
- 243
- 244 Cello G., Mazzoli S., Tondi E., Turco E., 1997. Active tectonics in the Central Apennines and possible
245 implications for seismic hazard analysis in peninsular Italy. *Tectonophysics*, 272, 43-68.
- 246
- 247 Cello G., Deiana G., Mangano P., Mazzoli S., Tondi E., Ferrelì L., Maschio L., Michetti A.M.,
248 Serva L., Vittori E., 1998. Evidence for surface faulting during the September 26, 1997,
249 Colfiorito (Central Italy) earthquakes. *Journal of Earthquake Engineering*, 2, 1-22.
- 250
- 251 Coltorti M., Farabollini P., 1995. Quaternary evolution of the Castelluccio di Norcia Basin. *Il*
252 *Quaternario*, 8, 149-166.
- 253
- 254 Galadini F., Galli P., 2000. Active tectonics in the Central Apennines (Italy) - Input data for
255 seismic hazard Assessment. *Natural Hazards*, 22, 225-270.
- 256
- 257 Galadini F., Galli P., 2003. Paleoseismology of silent faults in the central Apennines (Italy): the
258 Mt. Vettore and Laga Mts. faults. *Annali di Geofisica*, 46, 815-836.
- 259
- 260 Galvani, A., Anzidei, M., Devoti, R., Esposito, A., Pietrantonio, G., Pisani, A., Riguzzi, F.,
261 Serpelloni, E., 2012. The interseismic velocity field of the central Apennines from a dense GPS
262 network. *Ann. Geophys.* 55, 5, 2012; doi: 10.4401/ag-5634.
- 263
- 264 Gori S., Dramis F., Galadini F., Messina P., 2007. The use of geomorphological markers in the
265 footwall of active faults for kinematic evaluations: examples from the central Apennines.
266 *Bollettino della Società Geologica Italiana*, 126, 365-374.
- 267
- 268 Gruppo di Lavoro INGV sul terremoto in centro Italia (2016). Summary report on the October 30, 2016
269 earthquake in central Italy Mw 6.5, doi: 10.5281/zenodo.166238
- 270
- 271 Harris, R. A. Introduction to special section: Stress triggers, stress shadows, and implications for seismic
272 hazard. *J. Geophys. Res.* 103, 347–358 (1998).
- 273
- 274 EMERGEO Working Group (2016). Terremoto di Amatrice del 24 agosto 2016: Effetti Cosismici doi:
275 10.5281/zenodo.61566
- 276
- 277 Kilb, D., Gomberg, J. & Bodin, P. Triggering of earthquake aftershocks by dynamic stresses. *Nature* 408,
278 570–574 (2000).
- 279
- 280 Pierantoni P., Deiana G., Galdenzi S. Stratigraphic and structural features of the Sibillini mountain (Umbria-
281 Marche- Apennines, Italy). *Ital. J. Geosci. (Boll. Soc. Geol. It.)* Vol.132 No.3 (2013), pp. 497-520.



- 282
283 Pizzi A., Scisciani V., 2000. Methods for determining the Pleistocene–Holocene component of
284 displacement on active faults reactivating pre-Quaternary structures: examples from the central
285 Apennines (Italy). *Journal of Geodynamics* 29, 445–457.
286
287 Pizzi A., Calamita F., Coltorti M., Pieruccini P., 2002. Quaternary normal faults, intramontane
288 basins and seismicity in the Umbria-Marche- Abruzzi Apennine ridge (Italy): contribution of
289 neotectonic analysis to seismic hazard assessment. *Boll. Soc. Geol. It., Spec. Publ.*, 1,
290 923–929.
291
292 Pizzi A., Calamita F., Coltorti M., Pieruccini P., 2002. Quaternary normal faults, intramontane
293 basins and seismicity in the Umbria-Marche- Abruzzi Apennine ridge (Italy): contribution of
294 neotectonic analysis to seismic hazard assessment. *Boll. Soc. Geol. It., Spec. Publ.*, 1,
295 923–929.
296
297 Pizzi A., Galadini F., 2009. Pre-existing cross-structures and active fault segmentation in the
298 northern-central Apennines (Italy). *Tectonophysics*. 476, 304-319.
299
300 SUMMARY REPORT ON THE 30 OCTOBER, 2016 EARTHQUAKE IN CENTRAL ITALY Mw 6.5, Gruppo di Lavoro
301 INGV sul Terremoto in centro Italia 10 November 2016
302
303 Steacy, S., Gomberg, J. & Cocco, M. Introduction to special section: Stress transfer, earthquake triggering,
304 and time-dependent seismic hazard. *J. Geophys. Res.* 110, B05S01 (2005).
305
306 Stein, R. S. The role of stress transfer in earthquake occurrence. *Nature* 402, 605–609 (1999).
307
308
309 *Website link*
310
311 <http://iside.rm.ingv.it>
312
313 <http://ring.gm.ingv.it>
314
315 <http://www.igmi.org/geodetica/>
316
317 [http://www.irea.cnr.it/index.php?option=com_k2&view=item&id=761:nuovi-risultati-sul-terremoto-del-](http://www.irea.cnr.it/index.php?option=com_k2&view=item&id=761:nuovi-risultati-sul-terremoto-del-30-ottobre-2016-ottenuti-dai-radar-dei-satelliti-sentinel-1)
318 [30-ottobre-2016-ottenuti-dai-radar-dei-satelliti-sentinel-1](http://www.irea.cnr.it/index.php?option=com_k2&view=item&id=761:nuovi-risultati-sul-terremoto-del-30-ottobre-2016-ottenuti-dai-radar-dei-satelliti-sentinel-1)
319
320 <http://www.isprambiente.gov.it>
321
322 <http://www.unavco.org/software/data-processing/teqc/teqc.html>
323
324 Rete Integrata Nazionale GPS - <http://ring.gm.ingv.it/>